NASA-CR-199117

CANOPY REFLECTANCE MODELLING OF SEMIARID VEGETATION

NASA Grant NAGW-2031

FINAL REPORT

Janet Franklin
Principal Investigator

Submitted to the National Aeronautics and Space Administration

Reporting Period:
January 1, 1990 - December 31, 1994
Year 1: 1/1/90-12/31/90
Year 2: 1/1/91-12/31/91
Year 3: 1/1/92-12/31/92
Extension: 1/1/93-6/31/93
Year 4: 7/1/93-6/30/94
Extension: 7/1/94-12/32/94

Principal Investigator
Janet Franklin, Associate Professor
Department of Geography
San Diego State University
San Diego, CA 92182-4493
Telephone 619 594-5491
Fax 619 594-5642
E-mail janet@typhoon.sdsu.edu

Business Contact
Ms. Julie Marini
San Diego State University Foundation
5178 College Ave.
San Diego, CA 92182-1900
Telephone 619 594-1054
Fax 619 594-4950

CANOPY REFLECTANCE MODELING OF SEMIARID VEGETATION

FINAL REPORT

NASA Grant NAGW-2031
Janet Franklin, Principal Investigator

ABSTRACT

Three different types of remote sensing algorithms for estimating vegetation amount and other land surface biophysical parameters were tested for semiarid environments. These included statistical linear models, the Li-Strahler geometric-optical canopy model, and linear spectral mixture analysis. The two study areas were the National Science Foundation's Jornada Long Term Ecological Research site near Las Cruces, NM, in the northern Chihuahuan desert, and the HAPEX-Sahel site near Niamey, Niger, in West Africa, comprising semiarid rangeland and subtropical crop land. The statistical approach (simple and multiple regression) resulted in high correlations between SPOT satellite spectral reflectance and shrub and grass cover, although these correlations varied with the spatial scale of aggregation of the measurements. The Li-Strahler model produced estimated of shrub size and density for both study sites with large standard errors. In the Jornada, the estimates were accurate enough to be useful for characterizing structural differences among three shrub strata. In Niger, the range of shrub cover and size in short-fallow shrublands is so low that the necessity of spatially distributed estimation of shrub size and density is questionable. Spectral mixture analysis of multiscale, multitemporal, multispectral radiometer data and imagery for Niger showed a positive relationship between fractions of spectral endmembers and surface parameters of interest including soil cover, vegetation cover, and leaf area index.

PROJECT SUMMARY

This brief summary will outline the objectives and results of this research. A detailed description of the progress in the final year of the project can be found in the attached Appendix, outlining further work currently being carried out under sponsorship of a NASA Global Change Fellowship awarded to Jeffrey Duncan (doctoral candidate).

The objectives of the research funded under this award were to invert models of surface reflectance to estimate vegetation parameters from remotely sensed data, and specifically to examine the effect of woody cover (shrubs) on the composite spectral reflectance of semiarid landscapes composed of herbs, shrubs and bare soil. Our estimates of fractional cover and plant size will be used by our scientific collaborators as inputs to spatially disaggregated model of land surface-atmosphere exchanges of energy and water, and of ecosystem primary productivity. This work was carried out during the first two years of this NASA award in NSFs Jornada Long Term Ecological Research site, and in the last three years in conjunction with the HAPEX (Hydrologic-Atmospheric Pilot Experiment) - Sahel, that took place in Niger, West Africa during 1991-1992.

We are using spectral mixture and geometric optical models to estimate woody and herbaceous vegetation amount and soil cover at the subpixel level, and the size and density of shrubs at the multi-pixel stand level. We are examining the effects of sensor spatial,

spectral and temporal resolution on the estimation of these parameters using the rich HAPEX dataset consisting of ground-, aircraft- and satellite-based radiometric data and numerous field-based biophysical measurements.

This research will contribute to *a)* the physiologically-based modeling of primary production using satellite data, and *b)* the HAPEX goal of developing algorithms for deriving surface parameters that are important in land-atmosphere exchanges of energy and moisture from remotely sensed data in a subhumid tropical savanna.

Our results can be summarized as follows:

- The Li-Strahler geometrical-optical canopy reflectance model was inverted to predict shrub size and density in semidesert in New Mexico, USA (the Jornada Long Term Ecological Research site). While predictions had large average errors of 35%, estimates were reasonable (within one to 2 standard errors) when aggregated by shrub stratum. Parameterizing the non-random spatial pattern of shrubs in the model produced more accurate predictions (Franklin and Turner 1992).

- Empirical models were developed to predict shrub cover from broadband spectral reflectance and green vegetation indices in semidesert in New Mexico, USA (the Jornada Long Term Ecological Research site) using simple and multiple regression. Remotely sensed data were from the SPOT satellite. Coefficients of determination were as high as 0.77 despite a limited range of shrub cover in the sample. Greenness indices were more sensitive to shrub cover and phenology than brightness indices. The scale of aggregation for estimating both cover and reflectance had a substantial effect on the results. Shrub and grass cover could be differentiated using multidate SPOT imagery (Duncan et al. 1993).

- A broadband radiometer was used for field measurements of vegetation and soil components of the landscape in semiarid grassland and shrubland in New Mexico, USA (the Jornada Long Term Ecological Research site). Shaded components (self-shaded plant canopies and soil shaded by plant canopies) had distinct reflectances in the infrared band (due to strong scattering by green leaves) which affected spectral green vegetation indices for those components. Plant canopies of morphologically different shrub canopies had quite similar broadband optical reflectance properties at the end of the growing season, but could be distinguished temporally (Franklin et al. 1993).

- A cover-weighted spectral mixture model predicted the reflectance of two 0.5 km^2 sites from the cover and reflectance of shrubs and understory (grass and soil) in the tropical semiarid Sahel in Niger, West Africa. Ignoring the shaded components does not cause serious errors in the model (Duncan and Franklin 1993, Franklin et al. 1994)

- The Li-Strahler canopy reflectance model was inverted for 27 shrub fallow sites within the HAPEX-Sahel supersites. Predictions of shrub size and density had large average errors, but it was noted that the average and range of shrub cover in the sample sites was very low (about 4-15% cover; Duncan and Franklin 1993).

- A linear spectral mixture model was inverted for broadband radiometer data (Exotech) acquired from a light aircraft in conjunction with HAPEX-Sahel. Results showed a more temporally stable relationship for leaf area index than for projected canopy cover and green vegetation spectral fraction (Duncan and Franklin 1994).

SUMMARY OF PUBLICATIONS AND SUPPORT OF SCIENCE EDUCATION

All Refereed Publications Resulting from this Project

(Copies are enclosed, as noted, or have previously been submitted to NASA.)

Franklin, J., J. Duncan, A.R. Huete, W.J.D. van Leeuwen, X. Li and A. Begue, 1994, Radiative transfer in shrub savanna sites in Niger -- preliminary results from HAPEX-II/Sahel: 1. Modeling surface reflectance using a geometric-optical approach, *Agricultural and Forest Meteorology*, vol. 69, pp. 223-245.
(Copies enclosed per NASA reporting requirements.)

van Leeuwen, W.J.D., A.R. Huete, J. Duncan and J. Franklin, 1994, Radiative transfer in shrub savanna sites in Niger -- preliminary results from HAPEX-II/Sahel: 3. Optical dynamics and vegetation index sensitivity to biomass and plant cover, *Agricultural and Forest Meteorology*, vol. 69, pp. 267-288.
(Copies enclosed per NASA reporting requirements.)

Franklin, J., Duncan, J., and Turner, D.L., 1993, Reflectance of vegetation, soil and shadow in Chihuahuan desert plant communities from ground radiometry using SPOT wavebands, *Remote Sensing of Environment*, vol. 46, pp. 291-304.
(Copies enclosed per NASA reporting requirements.)

Duncan, J., D. Stow, J. Franklin and A. Hope, 1993, "Assessing the relationship between spectral vegetation indices and shrub cover in the Jornada Basin, New Mexico," *International Journal of Remote Sensing*, vol. 14, pp. 3395-3416.

Franklin, J., and Turner, D., 1992, The application of a geometric optical canopy reflectance model to semiarid shrub vegetation, *IEEE Tran. Geosci. Remote Sens.* vol. 30, pp. 293-301.

Conference Proceedings and Papers Presented at Professional Meetings

Duncan, J. and J. Franklin, 1994, "Estimating fractional vegetation cover at the subpixel scale in a semiarid region using a statistical mixture model and remotely sensed data," Proceedings of the International Geoscience and Remote Sensing Symposium, Pasadena, CA, Aug 8-12, 1994, IEEE, Piscataway, NJ, pp. 1046-1048.
(Copies enclosed per NASA reporting requirements.)

Duncan, J., 1994, "Recovery of land surface variables: estimating fractional vegetation cover using spectral mixture analysis," Second HAPEX-Sahel Investigators Meeting, November 14-16, 1994, METEO-FRANCE, Toulouse, France. (Oral presentation.)

Duncan, J., 1993, "Spectral mixture modeling of vegetation using variable spectrla and spatial resolution data," First HAPEX-Sahel Investigators Meeting, May 12-14, 1993, Toulouse, France. (Oral presentation.)

Duncan, J., and Franklin, J., 1993, "Estimating shrub size and density using an invertible canopy reflectance model in Niger, West Africa: HAPEX Sahel 92," Annual Fall meeting of the American Geophysical Union, San Francisco, CA, December 6-10, 1993. (Abstract only.)
(Copies enclosed per NASA reporting requirements.)

Duncan, J., and Franklin, J., 1993, "Estimating shrub size and density using an invertible canopy reflectance model in Niger, West Africa: HAPEX Sahel 92," Annual Fall meeting of the American Geophysical Union, San Francisco, CA, December 6-10, 1993. (Abstract only.)
(Copies enclosed per NASA reporting requirements.)

van Leeuwen, W.J.D., A.R. Huete, A. Begue, J. Duncan, J. Franklin, N.P. Hanan, S.D. Prince and J.L. Roujean, 1993, "Evaluation of vegetation indices for retrieval of soil and vegetation parameters at HAPEX-Sahel." Proceedings of the Pecora 12 Symposium, August 23, 1993.
(Copies enclosed per NASA reporting requirements.)

Franklin, J., and Duncan, J., 1992, Testing the Li-Strahler four-component canopy reflectance model in the HAPEX-II-Sahel shrub savanna sites using ground reflectance data, *Proceedings IGARSS '92*, pp. 200-202. (Poster presentation at IGARSS '92, May 26-29, 1992, Houston, TX.)

Franklin, J., and Turner, D.L., 1992, The application of a discrete object reflectance model to a semiarid shrub canopy, Annual Meeting of the Association of American Geographers, April 18-22, 1992, San Diego, CA (abstract only).

Franklin, J. and D. Turner, 1990, Modeling the reflectance of a desert shrub canopy, (a poster presentation) Ecological Society of America Annual Meeting, July/August 1990, Snowbird, Utah (abstract only).

Support for Scientific Education and Training

This grant supported scientific education and training by sponsoring the graduate research theses listed below. In addition, the opportunity to participate in field work (remote sensing, biophysical and ecophysiological field measurements) was provided for the following San Diego State University students:

- Amy Craddock (undergraduate, Geography)
- Michael Russo (Masters student, Geography)
- Joseph Shandley (Masters student, Geography)
- NaDene Sorensen (Masters student, Ecology)

Graduate Theses

Debra Turner, April 1991, "Geometric-optical canopy reflectance modeling of semiarid shrub vegetation," Masters Thesis, Geography, San Diego State University, San Diego, CA.

Jeffrey Duncan, 1991, "Assessing the relationship between spectral vegetation indices and shrub cover in a semiarid environment," Masters Thesis, Geography, San Diego State University, San Diego, CA.

Jeffrey Duncan, in progress, "Spectral mixture/geometric optical canopy modeling of surface components in a semiarid region," Doctoral Dissertation, Geography, San Diego State University, San Diego, CA (anticipated completion August 1995).

APPENDIX

SPECTRAL MIXTURE/GEOMETRIC OPTICAL CANOPY MODELING OF SURFACE COMPONENTS IN A SEMIARID REGION

A Dissertation Proposal by Jeffrey A. Duncan

Detailing the Progress in Year 4 of NASA Award NAGW-2031

and

Progress to Date, Year 1, NASA Global Change Fellowship Award 3653-GC94-0041

1. Introduction

Accurate predictions of the future global climate require more realistic representations of the earth's surface in global climate models (GCM) (Dickinson, 1984; Sellers et al., 1986, Henderson-Sellers 1990). The exchange of energy and mass between the terrestrial surface and the atmosphere plays a large role in determining global climate, a circumstance of particular current interest because of the increasing role of human populations in affecting landcover changes. Soil type, and vegetation type and structure affect energy and mass fluxes (H_2O and CO_2) by largely determining surface albedo, the partitioning of net radiation into sensible and latent heat flux, and the level of turbulent flux through the partial control of aerodynamic roughness (Dickinson, 1983; Garratt, 1992). The use of satellite-borne sensors to monitor the significant surface components of the terrestrial biosphere is an important part of current research efforts because of the spatial and temporal scales at which observations from space can be made (Sellers et al., 1990). A consistent objective of the recent major international studies of land/atmosphere interactions, e.g., HAPEX-MOBILHY (Andre et al., 1988), FIFE (Sellers et al., 1992), EFEDA (Bolle et al., 1993) and the recent HAPEX-Sahel experiment which took place in Niger, West Africa in 1991-1992 (Goutorbe et al., 1994), has been to develop algorithms that "connect satellite observed radiances with the actual physical variables needed for climate studies and modeling" (Sellers et al., 1990, p. 1429).

The goal of the HAPEX-Sahel experiment was to better characterize the contribution of the Sahelian region to the global climate (Goutorbe et al., 1994). The Sahel, like other semiarid regions that together make up approximately one-third of the terrestrial earth surface, is subjected to land degradation caused by increased utilization and/or drought. In semiarid regions, degradation can result in a change in the ratio of herbaceous to woody cover significantly affecting mass and energy fluxes (Schlesinger et al., 1990). For example, preliminary results from HAPEX-Sahel showed that the maximum rate of photosynthesis in the herbaceous layer fell more rapidly than that of shrubs through the course of a day. This is indicative of an earlier closing of stomata by grass and forbs as a result of high surface temperatures and reduced soil moisture in the upper layer. Shrubs were able to keep their stomata open longer because of their ability to tap deeper water sources (Goutorbe et al., 1994). Furthermore, roughness length and its influence on turbulence in the lower atmospheric boundary layer can vary significantly with large variations in the shrub cover/herbaceous layer ratio (Graetz, 1990; Graetz et al., 1994).

The surface components that affect mass and energy fluxes, primarily woody vegetation, the herbaceous layer and soil, are spatially distributed such that they comprise mixtures at the scale of the satellite measurement, particularly in semiarid areas. Spectral mixture models may enable the quantification of the proportions of materials that contribute to the signal recorded for individual image pixels (Huete, 1986; Smith et al., 1990; Roberts et al., 1993; Mertes et al., 1993). However, in many of the studies of semiarid vegetation to date, the validation of component "fractions" estimated by mixture models has been largely qualitative. Furthermore, the estimates of vegetation fraction have been most often related to proportional cover, either qualitatively or empirically through regression with field estimates. It is of interest, therefore, to investigate the quantitative relationships between mixture model vegetation fractions and biophysical parameters, i.e., proportional cover, leaf area index (LAI) or biomass. The spatial and spectral resolution of the remotely sensed measurements themselves may affect these relationships, as will the timing of the measurements, particular in terms of vegetation phenology.

Geometric-optical canopy models explicitly relate inter-pixel brightness variations in a satellite image to spatial variations in vegetation canopy structural parameters, e.g. size, shape, spatial pattern and density, and the resultant distribution of shadows (Li et al., 1986; Franklin et al., 1992). Estimates of canopy shape, size and density are useful in calculations of surface roughness length, an important parameter in flux models (Graetz, 1990; Graetz et al., 1994; Raupach, 1992; Tuzet et al., 1993; Bogh et al., 1993). One assumption of geometric-optical canopy models is that brightness variations in the remotely sensed data are driven primarily by spatial variations in tree or shrub structural parameters, and not by variations in the reflectance of the background (soil and the herbaceous layer). Because spectral mixture models may provide explicit information about the subpixel proportions of surface components including the background it may be possible to integrate the two approaches and improve the accuracy of shrub size and density estimates in areas of high variability in background reflectance.

The HAPEX-Sahel experiment produced an extensive dataset including field measurements of surface characteristics, areal fluxes, and multispectral, multiscale, multitemporal measurements of surface

radiance from ground, air and satellite based sensors. Using these data, spectral mixture and geometric optical canopy models driven be remotely sensed data will be used to investigate the following research questions:

1) Can a spectral mixture model be used to estimate the spatial distribution of key biophysical parameters, e.g. proportional cover, LAI or biomass, in the HAPEX-Sahel study area, and with what degree of accuracy?
2) Can temporal variations in the above biophysical parameters be monitored in the study area using spectral mixture models?
3) What are the effects of variations in sensor spectral, spatial and temporal resolution on the above questions?
4) Can the spectral mixture and geometric optical approaches be integrated to improve estimates of shrub size and density in the study area?

The results will be used to support related research efforts within HAPEX-Sahel including the modeling of net primary productivity (NPP) using the satellite derived normalized difference vegetation index (NDVI) (Prince, 1991), and a model of radiative transfer that explicitly accounts for interception by the woody layer (Begue et al., 1994). Furthermore, model output could help provide maps of the spatial distribution of biophysical parameters related to NPP, and energy, CO_2 and H_2O fluxes, for example soil, vegetation cover and roughness length, suitable for scaling up site-specific measurements made during the Intensive Observation Period (IOP) of HAPEX-Sahel to mesoscale and global models. Finally, the results will help indicate the sensitivity of the models to sensor spectral and spatial resolution, and to the temporal variations in the spatial distribution of vegetation and soil in the Sahel, thereby improving model applicability to semiarid regions in general.

2. Background

Most of the current efforts to monitor vegetation from space rely on spectral vegetation indices (SVI) that contrast the differential reflectance of vegetation in the red and near-infrared (NIR) wavebands with that of soil, where the magnitude of reflectance is typically similar in both wavebands (Tucker, 1979). SVIs, such as the Simple Ratio, NDVI and SAVI have been shown, in some studies, to correlate well with vegetation parameters such as proportional vegetation cover, LAI and biomass (Tucker, 1979). However, in studies of sparse vegetation, SVIs have been shown to be highly sensitive to variations in soil reflectance, solar zenith angle, viewing angle and atmospheric effects (Huete, 1989). The relationship between SVIs and vegetation is typically calibrated empirically, for example, by regression with field measurements, for imagery acquired on a single date (Foran, 1987, Graetz et al., 1982). Where vegetation and soil form mixtures within the field of view (FOV) of the sensor, as is typically the case in semiarid areas, establishing this relationship can be problematic (Duncan et al., 1993a).

Spectral mixture models offer a means of quantifying the proportions of green vegetation, non-photosynthetically active vegetation (NPV) and soil occurring within pixels resolved by satellite sensors. Mixture models can also be used to simultaneously correct satellite data for extraneous factors affecting the measurement unrelated to the surface materials (Adams et al., 1993). Therefore, they are powerful tools for deriving information from satellite data critical to the accurate modeling of surface processes.

2.1. Spectral Mixture Modeling

In spectral mixture modeling, pixel reflectance is modeled as a linear combination of the reflectance of the components in the ground resolution element weighted by their areal proportions. The number of individual components whose proportions can be accurately estimated within the mixed pixels of a remotely sensed image is based on the intrinsic dimensionality of the data. The dimensionality of a remotely sensed image is determined by, 1) the number of components and their relative proportions within the scene (which determines the magnitude of the component signal), 2) spectral differentiation between component signatures, 3) the number of wavebands over which measurements are made, and 4) the signal to noise ratio of the measuring sensor (Sabol et al., 1992; Adams et al., 1993). The number of resolvable components cannot exceed $n + 1$ (where n = number of bands) and is usually less than n.

Spectral mixture modeling involves solving linear models of the form:

$$d_{ik} = \Sigma\, r_{ij}\, c_{jk} + e_{ik} \qquad (1)$$

where d_{ik} is the measured response of spectral mixture, i.e., pixel k in waveband i, summed over the number of significant reflecting components in the pixel, r_{ij} is the reflectance of component j in waveband i, c_{jk} is the proportion of component j in pixel k and e_{ik} is an error or residual term (from Huete, 1986). The magnitude of model residuals are affected by spatial variations in atmospheric conditions, by solar illumination variations across the scene as a function of shadows and shade at all scales, and by sensor response variations (Adams et al, 1993). Stochastic variations in the spectral reflectance of the scene components also contribute to model uncertainty. The model can be solved through a least squares approach by having knowledge of r, the component spectra, and finding for c, component proportions such that the error term is minimized.

Pure component spectra are typically distributed in different locations around the extremes of the n dimensional spectral data cloud determined by the spectra of all the pixels in an image (Boardman et al., 1994). In the two-dimensional representation illustrated in Figure 1, a bright soil "endmember" is located in the high red and NIR reflectance corner of the plot, the green vegetation endmember is found in the low red, high NIR corner and shade is the darkest component in the scene. This data structure is analogous to the Tasseled Cap transformation of Crist et al. (1984). All the other data points represent pixels that are various combinations of the pure endmember spectra. If the spectra of a component of interest lies closer to the center of the n dimensional data cloud than the extremes it is more difficult to model directly using the mixture model approach. This is because pixels comprised of combinations of other components can spectrally mimic the component of interest.

The model thus described applies strictly to the linear case where the incoming solar radiation interacts with only one material before reaching the sensor. The validity of this assumption varies with surface material type and with the spectral band used in the measurement. For example, some portion of the incoming solar radiation in the NIR wavelengths is reflected by green vegetation, acquiring a partial vegetation "signal" in the process. Some of this radiation is scattered in the direction of the underlying soil imparting a vegetation component to the resulting soil "signal" that is reflected back to the sensor (Huete, 1987; Roberts et al., 1991). Violations of the linear assumption may not have serious consequences in situations where non-linearly reflected radiation contributes only a small amount to the total areally-averaged reflectance, e.g., in semiarid areas where vegetation is sparse (Smith et al. 1990, Franklin et al., 1994).

A spectral mixture model can be used to explicitly calculate variations in scene radiance due to atmospheric effects and sensor noise. First, image endmembers are located consisting of individual pixels composed entirely of a single component of the n number of components in the model (e.g., bare soil, green vegetation and shade). If "pure" pixels can not be located in the scene, pixels are chosen whose spectra indicate the presence of large proportional covers of the single components. Image endmember spectra are then calibrated or aligned with the spectra of target endmembers measured in the field or the laboratory using multiple regression (Smith et al., 1990). The differences between image endmember spectra and target endmember spectra, as expressed by the gain and offset of the regression equation, are ascribed to atmospheric effects and sensor noise.

Variable illumination across the image is modeled explicitly by the inclusion of a "shade" endmember. Shade is modeled as a combination of shadow and photometric shade, defined as the decrease in measured reflected radiance due to an increase in the angle of incidence of solar irradiance (Roberts, 1991). While variable shade proportions directly affect pixel reflectance, they are not typically of interest in terms of biophysical models. Shade proportions must, therefore, be reassigned to more important biophysical components, e.g., vegetation and soil. Where photometric shade dominates, shade can be reapportioned to soil and vegetation components weighted according to the proportions of these components as estimated by the original model. Difficulties arise in reapportioning the shade fraction when "shade" is dominated by shadow. Shadows can be cast by vegetation canopies predominately onto bare soil, or onto other canopies, making the reapportionment process more problematic (Adams et al., 1993; Roberts, 1991).

Adams et al. (1993) describe an approach where the spectral mixture model is solved in an iterative fashion, and images of calculated fractions and residuals are used as diagnostic tools to evaluate the model. The spatial distribution of residuals can indicate the presence of a material not included in the model or the use of incorrect spectral signatures for the targeted scene components. While fractions are constrained to

sum to 1, individual fractions can be > 1 or < 0 (Adams et al., 1993). The spatial distribution of "out of bounds" fractions can then be used to evaluate the model parameterization. For example, if the spectra used to model green vegetation were taken from a pixel with less than 100% vegetation cover, pixels with greater green cover will have calculated fractions > 1 and other modeled components will have calculated fractions of < 0. Pixels with superpositive green fractions may provide more appropriate green vegetation endmember spectra.

A modified factor analysis approach has also been used to solve the mixed pixel problem (Malinowski and Howery, 1980; Huete, 1986; Malinowski, 1991). Here, the measurements of the reflectance of mixed pixels are portrayed as the rows of a matrix with the samples in various wavebands displayed as the matrix columns. The raw data matrix D is then decomposed into the product of an abstract spectral signature matrix R and a proportions matrix C, i.e., $D = R\,C$ (Malinowski et al., 1980; Huete, 1986). The procedure is statistically similar to the least squares approach described above, however, it also includes a useful method for determining the number of significant scene components and a method for predicting values for portions of target component spectra not measured in the field or in the laboratory.

In modified factor analysis, the original data matrix is first decomposed into its n orthogonal principle components, each of which has a characteristic abstract spectral signature. A number of tests can be used at this point to determine the correct number of components, e.g., defining the intrinsic dimensionality of the dataset. The abstract spectra of the significant components are then rotated to conform to the real spectra of suspected components in a target transformation step. During this step, component spectra measured in the field or in the laboratory can be tested individually to determine if a suspected component is present in the spectral mixture. Furthermore, if a value for a particular bandwidth is missing from the "library" spectra of a suspected component, it can be predicted in the target transformation step. The procedure also includes a test of the statistical significance of adding additional components to the model (Malinowski, 1991).

Most of the recent interest in the mixture modeling approach can be attributed to the work of the group at the University at Washington (Adams et al., 1986; Smith et al. 1990, Mertes et al. 1993, Roberts et al., 1993; and others). Mixture models have been applied to data from the Airborne Visible-Infrared Imaging Spectrometer [AVIRIS] (20 m FOV-dependent on altitude, 224 bands), Thematic Mapper [TM] (30 m FOV, 6 visible and infrared bands), Landsat Multispectral Scanner [MSS] (80 m FOV, 4 bands) and the Advance Very High Resolution Radiometer [AVHRR] data (1 km FOV, 2 bands, visible and NIR). In the case of AVHRR data the dimensionality of the 2 band data was increased by utilizing multidate spatially registered data, and the model was used to distinguish broad cover classes, e.g. forest vs. non-forest (Quarmby, 1992).

A review of the results of the studies cited above indicates that the accurate detection and quantification of surface materials using spectral mixture models is not necessarily limited to high spectral resolution datasets. General classes of surface features, for example, vegetation or soil, have similar reflectance spectra. Therefore, an increase in spectral resolution does not necessarily increase the delectability of particular vegetation or soil types (Huete, 1986; Smith et al., 1990). However, the use of higher spectral resolution data can reveal narrow absorption bands that can be diagnostic of surface materials such as NPV (Roberts et al., 1993). The results of an analysis of simulated MSS, TM, and AVIRIS data indicated that component detectability increased with spectral resolution, but the increase was offset somewhat by a reduced signal to noise ratio for the highest spectral resolution data tested (Sabol et al., 1992). Furthermore, component detectability varied because of variations in component spectra and differences in sensor band positions and bandwidths, both in terms of modeled fractions and in the use of model residuals to detect components that were not directly modeled (Roberts et al., 1993; Sabol et al., 1992).

Increased spatial resolution does not necessarily result in an increase in the number of detectable components if there is not a concurrent increase in spectral variation (Adams et al., 1993). Spectral variation over space could also result in increased variation in model residuals (i.e., a poorly fit model) because of: 1) unmodeled spectrally distinct components, 2) stochastic variations in the spectral response of modeled components, and 3) the absence of modeled components (Sabol et al., 1992). Varying sensor spatial resolutions could result in differences in both the variance of model residuals and the accuracy of component fraction estimates. However, spectrally distinct landscape units composed of different suites of components could be modeled separately using prior image stratification.

Estimates of the proportions of surface features by mixture modeling may be more precise than field estimates. For example, vegetation cover is usually overestimated by field techniques, because gaps between branches and leaves are difficult to measure in the field (Smith et al. 1990). Mixture model estimates of green vegetation proportions have also been shown to be correlated with vegetation phenology (Smith et al. 1990). However, in studies of semiarid vegetation to date, the validation of component fractions estimated by mixture models has been largely qualitative, and quantitative validations have been limited by difficulties in obtaining concurrent ground measurements. Furthermore, there is a lack of integrated studies into the effect of variations in both the spatial and spectral resolution of the remotely sensed measurement on 1) the accuracy of component fraction estimates and 2) the precise biophysical parameter, i.e., proportional cover, LAI or biomass, to which vegetation fraction estimates are most closely related. While the studies to date are indicative of the potential of the spectral mixture modeling approach, there is a need for further rigorous testing and validation of results in order to bring the technique into the mainstream of remote sensing image processing methods.

2.2 Geometric-Optical Canopy Modeling

Estimates of vegetation size and density are necessary for an accurate calculation of aerodynamic roughness, which represents the level of turbulent coupling of the land surface to the atmosphere (Graetz, 1990; Graetz et al., 1994; Garratt, 1992). Much of the current research in modeling land/atmosphere exchanges of mass and energy at the GCM scale is focused on more accurate parameterization of the surface vegetative layer (Graetz et al., 1994). Geometric optical canopy models offer a means of deriving information about canopy size and density over large areas using remotely sensed data.

Geometric optical canopy modeling is a form of mixture modeling where pixel reflectance is modeled as a linear combination of the reflectance of four scene components: sunlit and shadowed canopy and background (a mixture of soil and herbaceous layer). The difference between the geometric optical model approach and the spectral mixture models described previously is that spatial variations in the proportional cover of the shadow components are explicitly modeled as functions of variations in canopy size and density. Spatial variations in background reflectance are assumed to have a minimal effect on the spatial variance in reflectance. A further assumption is that the spatial distribution function of shrubs is known or can be estimated in the field. Other parameters needed to run the model include estimates of the average shrub shape (estimated as the ratio of the horizontal to vertical radii of a shrub modeled as an ellipsoid) and the average spectral signatures of the sunlit and shaded crown and background components.

A key element in estimating crown size and density is the estimation of a cover index, m, calculated by,

$$m = \frac{nR^2}{A} \tag{2}$$

where n is the number of shrubs, R^2 is the average shrub diameter and A is area. Therefore, m is equal to shrub density times the average horizontal radius of the shrubs for a given area, in this case a single pixel. Multiplying m by π would yield an estimate of proportional shrub cover for a pixel. Li et al. (1985) show how m can be calculated solely on the basis of pixel reflectance, the signatures of the four components, and a geometric parameter relating the area of shrub crown and shadow, with shrub shape and the solar zenith angle. The cover index, m, can be calculated for each pixel in a stand. However, calculating m for a pixel does not automatically yield an estimate of size, given that many small shrubs and a few big shrubs can result in the same m value. However, if a homogeneous stand has many pixels, Li et al. (1985) proved that if the trees are randomly distributed within the stand, and crown size is independent of tree density, then:

$$R^2 \quad \frac{Vm}{(1+W)M} \tag{3}$$

where M and Vm are the mean and variance of m for all the pixels in a stand, and W is the coefficient of variation of the squared crown radius. Therefore, the mean shrub size for a stand is estimated from the

interpixel variance in m, the shrub cover index. Given m and R^2, equation 2 can be easily manipulated algebraically to yield an estimate of shrub density.

Model estimates of shrub size and density are problematic in semiarid areas because of the low density of shrubs and the lack of range in shrub cover which results in a low "signal" to noise ratio. The bright and variable background in these regions also contributes to noise unaccounted for by the model. One means of removing the influence of the background would be to derive an independent estimate of shrub cover on a pixel by pixel basis in a shrub stand through the use of a spectral mixture model. Shrub cover could then be easily converted to m for each pixel in a stand (described above). Then, using equations 3 and 2, R^2 could be calculated, as well as n, the number of shrubs per pixel in a stand.

The geometric optical canopy model approach has been used in coniferous forest (Li et al., 1985), tropical dry woodland and savanna (Franklin et al., 1988) and subtropical shrubland (Franklin et al., 1992) to estimate average plant crown size and density. Model estimates of shrub size and density in a semiarid desert in New Mexico were accurate to within 1-2 standard errors of the observed values (Franklin et al., 1992). These results indicated that it may be possible to categorize geometric optical model estimates of shrub size and density into reasonably accurate classes (Franklin et al., 1992).

3. Preliminary Research

Preliminary work related to the proposed research has already been completed, including field measurements at the HAPEX-Sahel study site, analysis of these data as they pertain to the implementation of the models, and a preliminary test of the geometric-optical canopy model. A description of the study area will be followed by a review of these preliminary results.

3.1 Study Area

The landscape of the study area, located in Niger, West Africa, consists of a fine scale patchwork of small-field millet production (field size $<< 1$ km^2) and fallow areas dominated by the deciduous shrub *Guiera senegalensis* and an herbaceous layer of annual grasses and forbs with some perennial grasses (Goutorbe et al., 1994). The millet and fallow fields occur predominately in wide sandy valleys separated by laterite-capped plateaus. The size of the irregularly shaped plateaus varies from < 1 km to an approximate maximum of 10 km along their long axes. Vegetation on the plateaus occurs as strips of dense shrubs and some trees, dominated by *Combretum micranthum*, *Combretum nigricans* and some *Guiera*, separated by bare laterite soil. Plateau vegetation is referred to as tiger bush because of the characteristic striping pattern evident in aerial photographs and remotely sensed imagery.

The HAPEX-Sahel experiment took place within on a 1° latitude x 1° longitude square (2-3° E, 13-14° N), comparable in size to a GCM grid cell, an area intended to encompass the spatial variability of the surface cover types described above. Three "super sites" selected for intensive study were located in an attempt to capture the long term north-south rainfall gradient of the region. Subsites representing the three major land cover strata, millet, fallow and tiger bush, were intensively studied within each of the super sites. While some data collection took place in 1991, the majority of the data were collected by all investigators in 1992, with an intensive observation period (IOP) from August 15 to October 9, 1992, timed to capture the transition from the wet to the dry season.

Rainfall, measured at gauges located throughout the 1° square, totaled an average of 537 mm for 1992 (Goutorbe et al., 1994). There was evidence of a significant north (low) to south (high) gradient in total rainfall. There was also a marked difference in the timing of rainfall over the study area with the southern super site receiving significant rainfall several weeks before the more northern super sites. Overall, there was evidence of extremely high frequency spatial and temporal variations in rainfall throughout the study area. The first rainfall was in late May with a marked increase from late July through August. After September 16 there was no measured rainfall within any of the supersites (Goutorbe et al., 1994).

The three to four month growing season in the region began with the onset of the summer monsoon in June-July and extended into October. The temporal cycle of vegetation green-up and senescence varied by vegetation type. During 1992, the deciduous shrubs began leaf growth in June followed by the growth of the herbaceous layer in July/August. The herbaceous layer green-up was temporally differentiated into two components, perennial grasses and annuals. Generally the growth of annual forbs appeared to precede the

new growth of perennial grasses by several weeks. The senescence of the annuals began in mid-September, six to eight weeks before that of the perennials. Shrubs did not begin to drop their leaves until after the IOP.

3.2 Field Measurements

During 1992, detailed field measurements of shrub size, density, spatial pattern and broad band component reflectances were made at two fallow subsites representative of the two main physiognomic types of shrub fallow in the region: *Guiera* with a perennial grass and annual grass and forb understory, and *Guiera* occurring on an eroded surface with little grass cover but with a large seasonal forb component. Average shrub size and shape was estimated by measuring two horizontal "diameters" (the longest axis of each shrub and the one perpendicular to it) and height for a number of shrubs in each of the two subsites. Sample shrubs were located by placing ten 15 m radius circular plots arranged in a regular grid through representative portions of each of the two plots (n = 344 and 288, for the shrub/grass and shrub/degraded sites, respectively).

The spectral signatures of the surface components in the shrub fallow subsites and tiger bush were sampled using a pole-mounted Exotech radiometer fitted with filters emulating the first four TM bands. The components sampled were sunlit and shaded shrub crown (and short trees in the tiger bush), the herbaceous layer (grass, forb), and soil (sand, eroded crust, laterite). In order to control for stochastic variations in reflectance among shrubs, twenty shrubs in each of the two detailed measurement plots were selected for repeated radiometric sampling. The component radiance measurements were converted to reflectance values using radiance measurements of a barium sulfate reflectance panel acquired periodically throughout each sampling session. Measurements were repeated at least once every two weeks from June to early October in order to evaluate the variations in component signatures with phenological changes and variations in solar zenith angle. During the sampling period from June to October, solar zenith angles at the time of measurement varied from 15° to 55° with a mean of 34° and standard deviation of 7.7°.

In order to better understand the variability, both spatially and temporally, of the reflectance of the background (herbaceous layer and soil), radiometric measurements were repeated at the fallow subsites approximately every two weeks along permanent 50 m transects (2 in each site). Each transect consisted of 50 contiguous 1 m x 1 m quadrats. Each quadrat was sampled radiometrically and visually interpreted for percentage cover of live and dead material. Qualitatively differences in soil color or relative soil brightness were recorded. The relative proportions of forb and grass cover was visually estimated.

Non-linear spectral mixing was investigated in the field by measuring the solar irradiance reaching the surface in TM bands 1-4 as a function of proximity to shrubs. The radiometer was fitted with diffusing 180° lenses and placed in an upward-looking orientation at the ground surface in sampling positions along transects near and under the 20 replicate shrubs in each of the two study plots. The sample transect, oriented along the solar plane, included 10 equally spaced samples beginning 2 m from a shrub on the side directly facing the sun with four samples 0.5 m apart, continuing with a sample under the leading edge of the shrub, 2 samples under the shrub canopy, 1 sample in the shrub shadow, and 2 samples in the sun beyond the shrub shadow. Upward-looking radiometric measurements were also made at ground level in more open areas (i.e., no shrubs within 20 m) before and after transect measurements for the purpose of standardizing the transect measurements. The measurements were made on four dates for each of the two subplots at approximately three week intervals.

3.3 Preliminary Results

3.3.1 Component Spectral Separability

An analysis of the component spectra indicated that the separability of some components varied temporally and was waveband specific. The four band spectra of most of the spatially significant surface components are displayed in Figure 2. The multiple samples displayed for each component are representative of variations in the spectra over the growing season. The earliest date displayed is July 30 (day of year [DOY] 212) when the shrub canopy in the sampled areas had increased to an average green leaf area index of 0.4 (Goutorbe et al., 1994). After this date there was less variance in the within component sampled spectra than between components.

The component spectra (Figure 2) showed significant spectral separation, predominately in the red and NIR bands but also in the green band. The three soil components, sand, eroded crust and laterite exhibited some differences in spectral curve shape but more significantly in the overall reflectance magnitude. Field observations showed that moisture content clearly affected soil reflectance, however, the surface layer of the predominantly sandy soils in the region dried quickly. When the eroded crust was moist it became spectrally more similar to laterite.

The spectra of the shrub crowns were indistinguishable from the shaded components in the visible wavelengths but all three components occupied different average positions in the NIR. The shadowed background component (the averaged spectra of shadowed soil and herbaceous layer) had the lowest NIR reflectance throughout the season, sunlit green vegetation the highest, while shadowed shrub crown had an average NIR reflectance value intermediate between the two. This can be attributed to increased NIR scatter by leaves within the canopy, resulting in a potentially unique canopy shade component (Roberts et al., 1993; Huete, 1986; Franklin et al., 1994).

The spectra of NPV, represented by samples of senescent grass standing in dense clumps are displayed in Figure 3 along with some of the previously displayed component spectra. The NPV spectra appeared to mimic that of laterite (shown in Figure 2) with slight variations in the red and NIR. As the ratio of green to senescent biomass in these clumps increased, their spectral response decreased in the visible bands and increased in the NIR until it approached that of green shrubs. This pattern was similar for both grass and forbs.

The results indicate that the number of spectrally unique and spatially significant components in the study area may exceed the maximum dimensionality of 3-6 band data. However, it may not be necessary to include all components in each mixture model because of variations in their spatial and temporal distributions. For example, when shrubs and the herbaceous layer both have an abundance of green leaves their spectra may be inseparable. However, it may be possible to model shrub and herb fractions at different times during the growing season when one type is "green" and the other is less "green". While the three soil components appear to exhibit unique spectra, it may not be necessary to include them simultaneously in the same model. For example, laterite is generally confined to the plateaus and the more degraded surfaces. Such surfaces could be modeled separately using prior image stratification. It may be possible to model NPV in areas with sandy soils but not where laterite predominates due to the similarity between NPV and laterite spectral signatures. Modeling shade as two separate components will be problematic because of sparse shrub cover and low amounts of shadow.

3.3.2 Non-linear Mixing

The measurements of surface irradiance near and under shrubs were standardized by ratio against the irradiance measurements taken in more open areas away from the influence of shrubs. Figure 4 illustrates a slight increase in the standardized NIR irradiance flux as a function of proximity to the shrub, an affect which is particularly noticeable when compared to the decrease in the standardized red irradiance flux. The net effect of this increase in NIR scatter, relative to red scatter, is to impart a shrub "signal" to the background near shrubs. In addition there was greater downward NIR flux, relative to downward red flux, within the shrub crown (positions 6 and 7 in Figure 4). These results are indicative of the degree of non-linear spectral interaction that could be expected to affect the model estimates of shrub and background fractions. However, the overall magnitude and effect of this non-linearity may not be great given the generally sparse shrub cover in the study area (Franklin et al., 1994).

3.4 Preliminary Geometric Optical Canopy Modeling

3.4.1. Areal Proportion Modeling: The Effects of Shadow and Shrub Transmission

As a first step towards evaluating the utility of the geometric optical canopy model for estimating shrub size and density in this landscape, the model was used to address the question: Can the average reflectance of a shrub stand be accurately modeled as the sum of the four component signatures (sunlit and shaded crown and background) weighted by their cover proportions? The study (described in detail in Franklin et al., 1994) utilized data acquired in 1991 at two 0.5 ha shrub fallow stands which were very

similar in cover type and proportions to the fallow sites sampled in the 1992 field campaign. The average site reflectances were modeled using component spectral signatures sampled in the field and component proportions estimated along 1000 m transects using the step-point method (Bonham, 1989). Average site reflectances were measured by averaging radiometric measurements acquired along 1000 m transects located adjacent to the cover transects. The areal proportions of site shadows were modeled using the mean sun angle at the time of the radiometric transect measurements, and the field estimated mean shrub shape, size and density. A model of photometric shade was not included in the test.

Average site reflectance was estimated using, 1) a two component model, including shrub crown and background but ignoring shadows, and 2) a four component model that included the shadowed components. The average site reflectances predicted by the two models were not statistically different, and both were in close agreement with the measured site reflectances (within .02-.04 reflectance units). Although the measured reflectances of shaded components were significantly darker than their sunlit counterparts, shrub crown cover and density were low in these sites, so that the shaded components had very small areas and contributed little to total surface reflectance (Franklin et al., 1994).

The spectral signatures of shrub crown and background, and estimates of shrub transmissivity (from Begue et al., 1994) were also used in a model of vegetation-soil spectral interaction modified from Huete (1987) to predict the spectral signatures of sunlit and shadowed shrub crown and shadowed background as a function of varying amounts of canopy closure (Franklin et al., 1994). As the modeled vegetation cover within a shrub crown was varied from 10 to 100%, red band reflectance decreased in a near linear fashion for all three components, and NIR reflectance decreased non-linearly for the two shadowed components and showed a slight increase for the sunlit crown. While this simulation could be validated for only 2 different crown cover amounts, it further illustrated the non-linearities associated with NIR scatter and variable green cover (Franklin et al., 1994).

3.4.2. Inverse Geometric Optical Canopy Modeling using SPOT Data

In order to parameterize a preliminary inversion test of the geometric optical canopy model and validate the estimates of shrub size and density, 27 shrub fallow stands (including the two fallow subsites intensively sampled in 1992) ranging in size from 2-10 ha were located in the study area using 1:14000 scale photography. The sample plots were first magnified and scanned with a high resolution CCD camera and brought into an image processing system. It was not possible to quantify the degree of magnification of the photographs, therefore the pixel size of the digitized photographs was estimated using control points from the original photographs of known scale. The average pixel size was 30 cm. In each plot, all shrubs were counted and measured using screen digitizing methods, a procedure enhanced by image processing techniques. A sample design analogous to the field methodology was used to estimate shrub size (average diameter only) and density for each plot. In order to test the validity of the estimates of shrub size and density obtained from the digitized photographs, the results were compared to shrub size and density estimates obtained in the field. The estimates of shrub size yielded by the field and air photo methodologies were not statistically different. The estimates of shrub density were also quite similar. These results are indicative of the validity of the estimates of shrub size and density estimated from the digitized photographs.

The geometric optical canopy model was used to estimate shrub size and density using data from the Systeme Pour l'Obvservation de la Terre (SPOT) sensor acquired on August 20, 1992, for the 27 fallow plots. At this time the shrubs were quite green and the herbaceous layer had not reached peak greenness. The individual SPOT bands were first transformed into brightness and greenness bands (Jackson, 1983). Brightness and greenness transforms have been found to increase the spectral differentiation between the four components of the model (Woodcock, pers. comm.). Shrub shape was parameterized as the average shrub radius to height ratio as measured in the field. An analysis of the aerial photos showed that the spatial distribution of shrubs was found to be equivalent to a Poisson distribution at the scale of a 20 m SPOT pixel.

Because the SPOT data used in this preliminary study had not been corrected for atmospheric effects it was not appropriate to use the component signatures measured in the field, or brightness/greenness transforms of those data, to run the model. Therefore, an iterative method was used to estimate the spectral signatures for sunlit and shadowed shrub crown and background (Woodcock et al., submitted). Briefly, sets of component spectral signatures were randomly chosen (within a spectral space constrained by theory and physical realism, for example, the sunlit crown signature must lie in the high greenness, low brightness

portion of the spectral space, soil in the high brightness, low greenness, etc.) and used to iteratively run the model producing estimates of the model index of shrub cover, *m*, for the 27 test fallow shrub stands. The optimal signature set chosen was the one that yielded an estimate of *m* closest to that estimated from the digitized photographs using the absolute difference in the two estimates as the criteria.

The model yielded unbiased estimates (i.e., the did not vary with the magnitude of the shrub size or density estimates) of shrub size and density, but with low accuracy (Duncan et al., 1993b). The sampled range of shrub cover used in the model was low (4% to 18%). A low range of shrub cover, combined with stochastic variability and high spatial variance in background reflectance may have resulted in a low "signal to noise" ratio. The range in shrub cover in this sample may simply be characteristic of fallow stands throughout the study area in which case the model may be poorly posed. A recently produced large-scale vegetation cover map of a small portion of one of the super sites may allow for the identification of fallow stands with higher proportions of shrub cover (Loireau et al., 1993 and Loireau, pers. comm.). Alternatively, the model could be reformulated to better account for background reflectance variations.

4. Proposed Research

4.1. General Approach

The HAPEX-Sahel experiment utilized a large array of sensors and platforms producing a diverse remotely sensed dataset (Goutorbe et al., 1994). Data were acquired throughout the growing season, with variable temporal coverage and frequency, by ground-based sensors (Exotech 4-Band Radiometer, SE-590 spectroradiometer), sensors on aircraft (Exotech 4-Band Radiometer, 50 m FOV; Thematic Mapper Simulator NS001, 6 bands in the visible and NIR, 3-15 m FOV dependent on altitude; Advanced Solid State Array Spectroradiometer [ASAS], 64 bands between 400 and 1060 nm, 3 m FOV) and satellite platforms (SPOT, 3 bands, 20 m FOV; TM, 6 bands in visible and NIR, 30 m FOV) in a multistage, multisensor, multidate approach. These data and extensive ground measurements of vegetation structure, spatial pattern, proportional cover and LAI made by a number of HAPEX investigators will be used to address the following research objectives.

4.2 Research Objectives and Hypotheses

The specific objectives of this study are to 1) use spectral mixture models to estimate the vegetation (including separate estimates of shrub and herbaceous layer fractions) and soil fractions in the shrub fallow, tiger bush and millet strata in the study area, with an accuracy comparable to field and air photo interpretation methods, 2) investigate the quantitative relationships between the estimated vegetation fractions and two biophysical quantities: proportional cover and LAI, 3) examine the effects of sensor spectral, spatial and temporal resolution on objectives 1 and 2, and 4) integrate the spectral mixture and geometric optical model approaches in order to improve the estimates of shrub size and density. A discussion of each hypothesis will be presented first.

1. The vegetation components in the study area are combinations of green, photosynthetically active plant parts, primarily leaves, and NPV, i.e., stems, branches and litter. In the study area, it is likely that the spectra of green leaves, soil and shade will constitute separable endmembers in the mixture model (i.e., their spectra will be located at different endpoints of the *n*-dimensional data cloud described by the remotely sensed data). The direct modeling of NPV may be problematic because of spectral similarities with soil, and soil/shade mixtures. Vegetation fraction estimates should be primarily correlated with green leaf abundance once the level of green leaf growth has achieved the minimum abundance for spectral detectability. Green vegetation fractions should also be correlated with proportional vegetation cover as vegetation leaf-out proceeds. However, the correlations should be greater with LAI, a more absolute measure of green leaf abundance. Green LAI was estimated in the field at shrub fallow and millet sites, but not in tiger bush, leading to the following hypotheses:

Hypothesis 1a: Correlations between green vegetation fractions and the proportional cover of actively photosynthesizing vegetation will be significant and positive for all three strata during the growing season after green LAI has achieved a level of abundance necessary for spectral detectability.

Hypothesis 1b: In the shrub fallow and millet strata, the correlations between modeled green vegetation fractions and LAI will be significantly greater than the correlations between modeled green vegetation fractions and proportional cover.

Hypothesis 1c: For shrub fallow and millet study plots, the slopes and intercepts of the green fraction/LAI relationships will be less variable over the course of the growing season than the slopes and intercepts of the green fraction/proportional cover relationships, which will vary seasonally with variations in the amount of green leaf material filling the plant crown volume.

2. While not spatially significant in the tiger bush and millet strata, the herbaceous cover is spatially abundant in the shrub fallow strata. However, it is not likely that shrubs and the herbaceous layer can be spectrally differentiated using a mixture model applied to broad band data (e.g., TM, NS001, SPOT, 4-band airborne sensor) when both vegetation types have an abundance of green leaves. However, it may be possible to estimate the relative cover proportions, or LAI, of shrubs vs. the herbaceous layer utilizing differences in their temporal pattern of green-up. The following hypotheses related to this objective are:

Hypothesis 2a: In shrub fallow stands, the correlation between green vegetation fractions estimated by spectral mixture models and shrub cover or shrub LAI will be significant and positive only early in the growing season, before the green-up of the herbaceous layer.

Hypothesis 2b: In shrub fallow stands, the correlation between green vegetation fractions estimated by spectral mixture models and the herbaceous layer proportional cover or LAI will be significant and positive for the period beginning when the herbaceous layer has achieved the minimum abundance for spectral detectability, until the period of herbaceous layer senescence at the end of the growing season.

3. The ability of a mixture model to detect and accurately estimate the fractions of particular surface components depends in part on the characteristic spectra of the component and the spectral characteristics of the sensor, e.g., the number of bands, the bandwidths, and their location along the electromagnetic spectrum. There may be some variation in component detectability among the tested sensors because of their variation in the above factors. For example, some of the bands sampled with the NS001 and TM sensors include narrow absorptive wavelength regions characteristic of leaf spectral properties (TM band 5), cellulose and lignin (TM band 7) (Elvidge, 1987). However, these component spectral properties may not be detectable within the wide bandwidths of the NS001 and TM sensors. The ASAS sensor detects radiance in many narrow bands but its coverage is limited to a spectral range between 400 and 1060 nm. These data, and the high spectral resolution measurements of component reflectance acquired in the field with the SE590 spectroradiometer, will be evaluated for potential narrow band absorptions that could be used to detect NPV, soil variations or to better differentiate shrubs from the herbaceous layer. The number of detectable components in the mixture can be estimated by the amount of variance explained by the model as a function of model complexity (e.g., the number of components in the model) leading to the following hypotheses:

Hypothesis 3a: The number of components in the mixture model resulting in the highest percentage of explained variance will not vary for the broad band sensors (e.g., from three to six bands).

Hypothesis 3b: For high spectral resolution ASAS data, the number of components in the mixture model resulting in the highest percentage of explained variance will be greater than the maximum number of detectable components for models of broad band data.

4. Variations in sensor spatial resolution should have an impact on spatial variations in model errors. Surface components with unique spectral signatures that cover small areas (for example, a contrasting vegetation or soil type) are typically not included explicitly in a mixture model, but do contribute spectral

noise to the model. Assuming a random spatial distribution for these components, high spatial resolution sensors will sample some pixels with high proportions of noise components and some pixels with low proportions of noise components (i.e., large interpixel noise variances). Low spatial resolution sensors averaging upwelling radiance over larger areas (i.e., larger pixel sizes) will tend to incorporate more equal amounts of noise components in each pixel (low interpixel noise variances). The residual error variances should follow this pattern since the residual error in the mixture model is simply the difference between modeled pixel reflectance (i.e., estimated fractions multiplied by their input spectral signatures) and measured pixel reflectance. The variance in the errors of the fractions should follow the patterns hypothesized above. It should, therefore, be possible to derive more accurate estimates of the spatial distribution of errors in fraction estimates from mixture models driven by high spatial resolution data than those derived from low spatial resolution data, even though their average errors are similar. The following hypothesis is proposed:

Hypothesis 4: Within a single landscape cover class, i.e., millet, fallow, or tiger bush, the highest spatial resolution data (smallest pixel size) will result in significantly greater interpixel variances in the residual error of the mixture model than that of the lowest spatial resolution data (larger pixel sizes).

5. In order to improve the accuracy of estimates of shrub size and density, output from the spectral mixture models (e.g., estimates of the subpixel proportions of shrubs, the herbaceous layer and soils) will be used in conjunction with a geometric optical canopy model. First, if an accurate estimate of shrub proportional cover can be derived from a spectral mixture model, then the average shrub size and density can be calculated directly using equations 2 and 3 from the geometric optical model (as described in section 2.2). Alternatively, an estimate of the variability in background reflectance could be derived. For example, the soil fraction estimated by the spectral mixture model for each pixel, multiplied times the soil spectra, would produce an estimate of the contribution of soil reflectance to the total reflectance of each pixel. Then, an estimate of the variance in soil reflectance for the shrub stand could be calculated. The same calculations could be done for the herbaceous layer. The stand reflectance variance due to the background could then be subtracted from the total stand variance leaving the reflectance variations due to shrubs and shadow to drive the geometric optical canopy model. Because of the spectral similarity of green shrub leaves and green herbaceous material, the accurate estimation of the herbaceous layer fractions may be problematic. However, given the magnitude of the soil reflectance and the spatial distribution and size of bare soil patches, as observed in the field, lessening of the influence of soil reflectance variations alone could improve the accuracy of the estimates of shrub size and density. Therefore, the following hypotheses are proposed:

Hypothesis 5a: The use of an independent estimate of shrub proportional cover from a spectral mixture model, in a modified version of the geometric optical canopy model, will result in a statistically significant improvement in the accuracy of estimates of shrub size and density over the estimates produced by an unmodified geometric optical canopy model.

Hypothesis 5b: The use of an independent estimate of soil proportional cover from a spectral mixture model, in a modified version of the geometric optical canopy model, will result in a statistically significant improvement in the accuracy of estimates of shrub size and density over the estimates produced by an unmodified geometric optical canopy model.

5. Methods

The proposed methodology of this dissertation (illustrated in Figure 5) will be described in four parts: 1) the acquisition and processing of both the radiometric and photographic data acquired from the Piper aircraft platform, described conjointly because of the interdependence of these two datasets, 2) the acquisition and preliminary processing of the other remotely sensed datasets, 3) the acquisition and processing of the field data and aerial photographic data necessary for parameterizing and validating the models, and 4) the proposed modeling sequence and analyses of results as they pertain to each hypothesis.

5.1 Airborne Four Band Radiometer Data and 35 mm Photography

Exotech radiometer data with a nominal 50 m FOV and concurrent 1:800 scale 35 mm photographs were acquired by researchers aboard a Piper light aircraft. The Piper was used to intensively sample the millet, fallow and tiger bush subsites in all three super sites taking repeated measurements along short transects across each subsite. The sample design resulted in 10 to 20 non-overlapping measurements per measurement date across a subsite. In addition, measurements were taken periodically along longer transects across portions of the 1° square (n = 50-100). The acquisition of Piper data commenced prior to the onset of the growing season and continued at approximately two week intervals until mid-October, just before complete vegetation senescence. The samples of surface radiance have been converted to reflectance factors using data from a cross-calibrated Exotech concurrently sampling the reflectance of a reference plate on the ground (Wim van Leeuwen, pers. comm.).

The proportional cover of the components within the radiometric FOV of each sample will be determined by an analysis of each accompanying photograph. The location of the FOV within the photographs will have to be estimated at the outset of the analysis because the alignment of the radiometer relative to the alignment of the camera was not precisely determined during the period of data acquisition. The radiometer FOV will be located by analyzing photographs that contain varying amounts of surface components with highly contrasting radiometric signals. For example, a series of samples acquired along a transect over the Niger river contained different amounts of a lush, green, rice crop and open water, two cover types with contrasting pure radiometric signatures. A radiometric signal conforming to the spectra of water would indicate that the entire FOV was within the portion of the photograph delimited by water. As the relative amounts of water and rice cultivation vary in the photographs, the radiometric signal will vary in accordance with the location of the radiometer FOV, enabling the determination of the approximate location of the radiometric footprint.

Once the location of the FOV has been determined, the proportional cover of the components (vegetation, soil) within each sample will be estimated from each accompanying photograph using the dot grid method (Duncan et al., 1993a, Warren et al., 1986). The photographs will be projected over a grid of dots with a resolution of approximately 1 m. The vertically projected cover of each component will then be estimated as the ratio of the number of dots intersecting each component divided by the total number of dots in the grid, multiplied by 100. Different vegetation types, soil color and NPV will be scored as separate components if distinguishable in all the photographs for any particular date/flight.

5.2 Other Remotely Sensed Datasets

NASA scientists aboard a C-130 aircraft acquired NS001 and ASAS data periodically during the IOP, from August 15 to October 9. These data were acquired over all subsites along short imaging transects. There were additional data acquisitions along longer transects across the 1° square. The pixel size of the NS001 images varied from 2 to 20 m depending on the flying height. The pixel size of the nadir look ASAS images was nominally 3 m. The NS001 and ASAS data are undergoing radiometric and atmospheric correction (using the 6S model described in Didier et al., 1993) by researchers at NASA Ames and NASA Goddard, respectively.

Four, cloud-free TM scenes were acquired in a sporadic temporal sequence, beginning before the start of the growing season (June 5), during or just after the peak of the growing season (September 25 and 26) and after peak greenness but before complete senescence (October 14). These data are undergoing atmospheric correction and calibration to reflectance values (M. Spanner NASA Ames, pers. comm.). Fifteen SPOT images were acquired with high temporal frequency during the 1992 growing season. The SPOT images have been corrected for atmospheric effects using the radiative transfer model 6S and calibrated to reflectance values by HAPEX-Sahel researchers working at LERTS in France (Kerr, pers. comm.).

5.3 Field Data and Aerial Photography

Most of the field data collection procedures have already been described (see Section 3.2). In addition to the two fallow plots studied extensively in the field, 25 additional fallow plots have been identified in the aerial photographs acquired by researchers aboard NASA's C-130 aircraft (see Section

3.4.2). The average shrub size (vertical dimensions) and density of these plots has been estimated. The proportional cover of soil and the herbaceous layer will also be estimated for these plots using the dot grid method (Duncan et al., 1993a and see Section 5.3 above). An additional 20 study plots within the tiger bush strata will be identified in the aerial photography and analyzed for the proportional cover of vegetation and soil using the dot grid method. Component cover and LAI was also estimated at all fallow and millet subsites throughout the growing season at approximately monthly intervals by other investigators (Prince et al., 1993; Goutorbe et al., 1994).

The acquisition of component signatures in the first four TM bands via handheld radiometer has been described previously (see Section 3.2). Samples of component spectra were also acquired with a SE590 spectroradiometer (described in van Leeuwen et al., submitted). These data will be evaluated for potential narrow band absorptions that could be used to detect NPV, multiple soil types or to better differentiate shrubs from the herbaceous layer using ASAS data.

6. Modeling

6.1 Spectral Mixture Modeling

In this section, the initial parameterization of the mixture models will be discussed first, followed by a description of the model outputs and how they will be used to test Hypotheses 1-4 (e.g., the hypotheses related most directly to spectral mixture modeling.) Finally, the modeling procedures related to testing Hypothesis 5 (integrating the mixture model outputs with the geometric optical canopy model) will be discussed.

6.1.1 Mixture Analysis Parameterization and Initial Evaluation

A linear spectral mixture analysis will be performed for each remotely sensed dataset (e.g., Piper four band radiometer, SPOT, NS001, TM and ASAS) acquired on each date throughout the growing season. Each model tested will include a minimum of three components (green vegetation, soil and shade). More complex models including additional components, for example NPV and/or multiple soil types, will be tested with data having six or more bands (e.g. NS001, TM and ASAS). Each mixture model will be evaluated initially by, 1) the amount of spectral variance in the input data explained by the model (i.e., are the components in the model the major source of the spectral variance), 2) the magnitude and spatial distribution of the model residuals, and 3) the relative magnitudes and spatial distribution of the component fraction estimates.

Mixture analyses of the Piper radiometer data will be fit using component four band reflectances measured in the field. The high spatial resolution datasets (e.g., NS001 and ASAS) are likely to contain pixels consisting of pure components, therefore, these mixture models will be fit using image endmember spectra alone. Identifying single pixels in the SPOT or TM imagery that are composed of pure components will be problematic leading to alternative parameterization methodologies.

The SPOT images used in the mixture analysis will have undergone atmospheric correction and an independent calibration to reflectance values. Therefore, the initial modeling of these data will utilize component reflectances measured in the field. This will involve converting component reflectances measured in TM bands 2, 3 and 4 (green, red and NIR) with their SPOT equivalents. In order to derive the correct conversion factors, the reflectance of the reference plate was sampled in the field with the radiometer fitted alternatively with the corresponding TM and SPOT filters.

If the initial evaluation of the mixture model indicates that the atmospheric correction of the SPOT data may be incomplete, reference endmembers will be aligned to image endmembers using the two-step approach (Smith et al., 1990; Roberts et al., 1993). First, image endmembers will be chosen that have high proportional covers of each component in the model, but do not necessarily represent pure pixels of the single components. These endmember spectra will then be modeled, using multiple regression, as combinations of the reflectance spectra of the suspected components in the model as measured in the field. The coefficients of the regression will be used to further correct the satellite data for atmospheric effects and recalibrate the data to reflectance values. The mixture analysis will then be repeated using the field-measured component reflectances.

The TM images are also undergoing atmospheric correction and calibration to reflectance values. However, the radiometric sensors used in the field did not sample beyond 1160 nm. Therefore, there are no estimates of component reflectances in TM bands 5 and 7. The initial mixture analyses will utilize image endmembers. The results of these analyses will be assessed and if they prove unsatisfactory, the factor analysis approach will be utilized in order to predict component reflectances in the unsampled spectral bands. First, the data matrix of samples (pixels) by bands will be decomposed into its abstract eigenspectra and eigenvector matrices using singular value decomposition. At the same time, the singular values of the matrix will be produced, yielding an estimate of the variance explained by each abstract component. Then, the eigenspectra of the significant components will be aligned with the reflectance spectra of the real components at which time the missing band samples will be simultaneously predicted (Malinowski, 1991). The transformation matrix used to align the component spectra will be applied to the eigenvector matrix producing the real fractions. The model residuals will then be calculated on a pixel by pixel basis.

6.1.2 Testing Hypotheses

In order to test hypotheses 1 and 2, vegetation fraction estimates will be regressed against proportional vegetation cover estimated in the field and from aerial photographs for all three vegetation strata (fallow, millet and tiger bush), and against LAI estimated in the field at the fallow and millet subsites. For fallow data, regressions will be run separately for shrubs and the herbaceous layer, and for these two vegetation types combined. Vegetation fraction estimates from the mixture analysis of the Piper radiometer data will be regressed against vegetation cover estimates on a sample by sample basis for each date and cover type. Regressions against LAI estimated at the subsite level will done using reflectance data averaged over the subsite. For the remotely sensed data in image format, vegetation fractions will be extracted for each subsite and all additional study plots identified in the aerial photography. The average fraction for each plot will be regressed against cover or LAI for each sensor/image type, date, and vegetation strata.

LAI was estimated at approximately monthly intervals only at the fallow and millet subsites (n = four and three, respectively). Therefore, a regression analysis of the fraction/LAI relationships for a single date will be problematic because of the small number of samples. An additional analysis will utilize the complete temporal sequence of LAI estimates in regressions against the vegetation fraction estimates. This analysis will be done for the millet and fallow strata (the shrub and herbaceous layer separately, and combined), for each of the remotely sensed data types.

Hypothesis 3, component "detectability" as a function of spectral resolution, will be tested by comparing the number of components in each mixture model resulting in the highest percentage of explained variance. In addition, the level of correlation of fraction estimates with the corresponding field and photographic estimates of vegetation and soil cover will be evaluated as a function of model complexity (number of components) and remotely sensed data type.

Hypothesis 4 will be tested by comparing the variance in model residuals for mixture models of varying spatial resolution data acquired on similar dates. Furthermore, the semivariance of the residuals (both the residual averaged across all bands and for each individual band) for each plot within each strata will be calculated and analyzed for spatial structures that could be indicative of the source of model errors, e.g., unmodeled components, or incorrect component signatures. Finally, the spatial distribution of negative residuals will be analyzed as a means of identifying unmodeled components, e.g., NPV, that exhibit characteristic absorptions within particular spectral bands.

6.2 Geometric Optical Canopy Modeling

As described previously, the geometric optical canopy model has been tested in shrub fallow areas using one date of SPOT data with the results validated using the estimates of shrub size and density from 27 shrub fallow study plots. Further tests of the model will be conducted using additional dates of atmospherically corrected SPOT and TM imagery. The component signatures used in these tests will be determined in two ways. First, using 14 of the 27 fallow study plots (leaving 13 plots for model evaluation) the iterative method described previously for uncorrected data will be used (see sections 2.2 and 4.3). The aerial photography and the vegetation map (Loireau, pers. comm.) of a small portion of one of the super sites will be examined for fallow stands with larger or more dense shrubs to improve model calibration. An

additional test of the model will use the field measured component signatures directly in models of satellite data that have been calibrated to reflectance values.

Hypothesis 5 will be tested in the following ways. First, if an accurate estimate of shrub proportional cover can be derived from a spectral mixture model (see Hypothesis 2a), then the average shrub size and density will be calculated directly. Shrub cover will be converted to the cover index, m, by dividing by π on a pixel by pixel basis. Then, the mean and variance of m for each test stand will be used to calculate R^2, or the average shrub size per stand using equation 3. Equation 2 will then be manipulated algebraically to solve for n yielding an estimate of density for each pixel in each stand.

Alternatively, an estimate of the variability in the stand background reflectance will be derived by multiplying the fractions of background components estimated by the mixture model, by their respective spectra. The stand background reflectance variance will then be subtracted from the total stand variance leaving the reflectance variations due to shrubs and shadow to drive the geometric optical canopy model. If an accurate estimate of the herbaceous layer fraction cannot be produced by the mixture model, the same procedure will be followed for the soil fraction alone. Given the magnitude of the soil reflectance and the spatial distribution and size of bare soil patches, the lessening of the influence of soil reflectance variations may improve the accuracy of the estimates of shrub size and density.

The estimates of shrub size and density from the unmodified and modified geometric optical canopy models will be validated by regression against the estimates of density and size (shrub diameters) for all 27 fallow study plots where size and density has been estimated in the field and from aerial photographs.

7. Anticipated Results and Discussion

The ultimate goal of this study is to use spectral mixture models and a geometric optical canopy model to estimate the spatial distribution of key biophysical parameters needed for climatological models of surface flux, NPP models, and for studies of land cover changes over time, in the semiarid sub-Sahelian biome. The HAPEX-Sahel dataset, including extensive ground, air and satellite measurements, affords the opportunity for an integrated study of the effects of sensor spatial, spectral and temporal resolution on the kinds of biophysical parameters that can be estimated, and with what degree of accuracy in this landscape type. The significance of the anticipated results of this study will be discussed within the framework of the research hypotheses.

The results pertaining to hypotheses 1a. and 1b. will help clarify the link between modeled vegetation fractions and the biophysical parameters, proportional cover and LAI. Using green vegetation endmembers in the mixture model should result in fractions that are significantly correlated with the proportional cover of the actively photosynthesizing vegetation, even though the estimation of proportional cover includes NPV, shade and small canopy gaps. Correlations should be greater with a pure measure of photosynthetic material, e.g., green biomass or LAI. Furthermore, the slopes and intercepts of this relationship should be more constant over time, leading to the potential for the development of empirically derived equations for predicting LAI from mixture model green vegetation fractions based on future or retrospective imagery.

Using broad band data in a spectral mixture model to differentiate shrub fractions from herbaceous layer fractions in shrub fallow areas will be problematic, particularly when both shrubs and herbs have an abundance of green leaves. However, utilizing the temporal variability in their respective patterns of leaf-out and senescence (Hypotheses 2a. and 2b.), it may be possible to derive an estimate of their relative proportions. Furthermore, an estimate of the proportional cover of shrubs made before the start of the growing season could be used as an initial condition in models of NPP. An early growing season estimate of shrub LAI (before the green-up of the herbaceous layer) could also be used to help calibrate an NPP model.

Increasing the number of spectral bands may not result in an increase in component detectability (i.e., greater number of components) or in the accuracy of component fraction estimates (Hypothesis 3). However, the results may show that mixture models using data from a variety of broad band sensors can estimate the fractions of the dominant surface components with reasonable accuracy. Broadband satellite sensors provide the necessary data for current large-scale studies of earth surface processes, and were also used to acquire the historical data necessary for studies of landcover changes that may have already taken place. The analysis of high spectral resolution data may show an increased capability to detect a greater

number of components, either through direct modeling or residual analysis. This result could be further evidence for the need for high spectral resolution sensors on satellite platforms.

As stated in the discussion of Hypothesis 4, variations in sensor spatial resolution should have its greatest impact on spatial variations in model errors. Higher spatial resolution should result in more individual pixels with higher proportions of unmodeled components, or other "noise" factors, resulting in higher interpixel error variance. Larger pixels should incorporate more constant amounts of noise in each pixel resulting in lower interpixel error variance. The relationship between spatial resolution and the variable inclusion of noise in the model will more importantly impact the accuracy of the modeled fraction estimates. It might, therefore, be possible to derive more accurate estimates of the spatial distribution of errors in fraction estimates from mixture models driven by high spatial resolution data than those derived from low spatial resolution data, even though their average errors might be similar.

Finally, combining the spectral mixture and geometric optical approaches (Hypotheses 5a. and 5b.) may result in increased accuracy in the estimates of shrub size and density. The spectral mixture model may provide a method for estimating shrub cover, from which shrub size can be calculated directly using a modified form of the geometric optical canopy model. Alternatively, the mixture model could provide estimates of the cover of background components on a pixel by pixel basis. The variance in background reflectance could then be calculated and removed from the stand reflectance variance leaving that due primarily to shrubs and the shadows they cast to run the geometric optical canopy model. Thus, improved estimates of the spatial distribution of shrub size and density could be calculated and used to help parameterize roughness length estimates in flux models.

References

Adams, J. B., Smith, M. O., and Johnson, P. E., 1986, "Spectral mixture modeling: a new analysis of rock and soil types at the Viking Lander 1 site," Journal of Geophysical Research 91(B8):8098-8112.

Adams, J. B., M. O. Smith and A. R. Gillespie, 1993, "Imaging spectroscopy: Interpretation based on spectral mixture analysis", In: Remote Geochemical Analysis: Elemental and Mineralogical Composition, C. M. Pieters and P. A. J. Englert Eds., Cambridge University Press, 145-166.

Andre, J-C., and others, 1988, "Evaporation over land surfaces: first results from HAPEX-MOBILHY special observing period," Annals Geophysica 6: 477-492.

Begue, A., N. P. Hanan and S. D. Prince, 1994, "Radiative transfer in shrub savanna sites in Niger--First results of HAPEX-Sahel. 2. Photosynthetically active radiation interception of the woody layer," Agriculture and Forest Meteorology 69: 247-266.

Boardman, J. W., 1994, "Geometric mixture analysis of imaging spectrometry data," IGARSS'94, Surface and Atmospheric Remote Sensing: Technologies, Data Analysis and Interpretation vol. 4:2369-2371.

Bogh, E. and H. Sogaard, 1993, "Interaction between landform, vegetation and water balance in the Sahel," EOS, Transactions, American Geophysical Union, 1993 Fall Meeting, Vol. 74(43):232.

Bolle, H-J., J-C. Andre and 34 others, "EFEDA: European Field Experiment in a Desertification threatened Area," Annals Geophysicae 11:173-189.

Bonham, C. C., 1989, Measurements for Terrestrial Vegetation, Wiley, New York, 338 pp.

Chavez, P. S. (1989), "Radiometric calibration of Landsat Thematic Mapper multispectral images," Photogrammetric Engineering and Remote Sensing 55:1285-1294.

Crist, E. P., and R. C. Ciccone, 1984, "A physically-based transformation of Thematic Mapper data--the TM Tasseled Cap," IEEE Transactions on Geoscience and Remote Sensing 26 (6):809-925.

Dickinson, R. E., 1983, "Land surface processes and climate-surface albedos and energy balance," Advances in Geophysics, Vol. 25, Academic Press, 305-353.

Dickinson, R. E., 1984, "Modeling evapotranspiration for three- dimensional global climate models," In: Climate Processes and Climate Sensitivity (Geophysical Monograph 29, Maurice Ewing Vol. 5) American Geophysical Union, Washington, D. C., 58-72.

Duncan, J. A., D. Stow, J. Franklin and A. Hope, 1993a, "Assessing the relationship between spectral vegetation indices and shrub cover in the Jornada Basin, New Mexico," International Journal of Remote Sensing 14(18):3395-3416.

Duncan, J. A. and J. Franklin, 1993b, "Estimating shrub size and density using an invertible canopy reflectance model in Niger, West Africa: HAPEX Sahel 92," EOS, Transactions, American Geophysical Union, 1993 Fall Meeting, Vol. 74(43):253.

Elvidge, C. D., 1987, "Reflectance characteristics of dry plant material," in Proceedings 21st International Symposium on Remote Sensing of Environment, Ann Arbor, Mi, 26-30 Oct., 13 pp.

Foran, B. D. (1987), "Detection of yearly cover change with Landsat MSS on pastoral landscapes in Central Australia," Remote Sensing of Environment, 23:333-350.

Franklin, J. and A. H. Strahler, 1988, "Invertible canopy reflectance model of vegetation structure in semiarid woodland," IEEE Transactions on Geoscience and Remote Sensing GE-26: 809-825.

Franklin, J. and D. L. Turner, 1992, "The Application of a geometric optical canopy reflectance model to semiarid shrub vegetation," IEEE Transactions on Geoscience and Remote Sensing 30(2): 293-301.

Franklin, J., J. Duncan, A. R. Huete, W. J. D. van Leeuwen, X. Li, and A. Begue, 1994, "Radiative transfer in shrub savanna sites in Niger: preliminary results from HAPEX-Sahel. I. Modeling surface reflectance using a geometric-optical approach," Agricultural and Forest Meteorology 69: 223-245.

Garratt, J. R., 1992, The Atmospheric Boundary Layer, Cambridge, Cambridge University Press, 316 pp.

Graetz, R. D., and M. R. Gentle, 1982, "The relationships between reflectance in the Landsat wavebands and the composition of an Australian semi-arid shrub rangeland," Photogrammetric Engineering and Remote Sensing 48:1721-1730.

Graetz, R. D., 1990, "Remote sensing of terrestrial ecosystem structure: an ecologist's pragmatic view," in Remote Sensing of Biosphere Functioning, Springer-Verlag.

Graetz, R. D., and M. A. Wilson, 1994, "Characterising the landcover of the Australian continent for incorporation into high spatial resolution GCMs," IGARSS'94, Surface and Atmospheric Remote Sensing: Technologies, Data Analysis and Interpretation vol. 1:178-180.

Goutorbe, J-P, T. Lebel, A. Tinga, et al., 1994, "HAPEX-SAHEL: A large scale study of land-atmosphere interactions in the semi- arid tropics," Annals Geophysica 12:53-64.

Henderson-Sellers, A., 1990, "The "coming of age" of land surface climatology", Palaeogeography, Palaeoclimatology, Palaeoecology (Global and Planetary Change Section) 82: 291-319.

Huete, A. R., 1986, "Separation of soil-plant spectral mixtures by factor analysis," Remote Sensing of Environment 19: 237-251.

Huete, A. R., 1987, "Soil-dependent spectral response in a developing plant canopy," Agronomy Journal 79:61-68.

Jackson, R. D. (1983), "Spectral indices in n-space," Remote Sensing of Environment 13:409-421.

Li, X. and A. H. Strahler, 1985, "Geometric-optical modeling of a conifer forest canopy," IEEE Transactions on Geoscience and Remote Sensing, GE-23(5):705-721.

Loireau, M. and J. M. d'Herbes, 1993, "Mapping of land features over the HAPEX Sahel East Central Super Site (ECSS)", EOS, Transactions, American Geophysical Union, 1993 Fall Meeting, Vol. 74(43):231.

Malinowski, E., R., 1991, Factor Analysis in Chemistry, 2nd. Edition, Wiley, New York.

Malinowski, E. R. and D. G. Howery, 1980, Factor Analysis in Chemistry, Wiley, New York.

Mertes, L. A. K., M. O. Smith and J. B. Adams, 1993, "Estimating suspended sediment concentrations in surface waters of the Amazon River wetlands from Landsat Images," Remote Sensing of Environment 43:281-301.

Mustard, J. F., 1993, "Relationships of soil, grass, and bedrock over the Kaweah Serpentinite Melange through spectral mixture analysis of AVIRIS data," Remote Sensing of Environment 44: 293- 308.

Prince, S. D., 1991, "A model of regional primary production for use with coarse-resolution satellite data," International Journal of Remote Sensing 12:1313-1330.

Prince, S. D., N. P. Hanan and A. Begue, 1993, "Vegetation primary production efficiency on the West Central Site during HAPEX-Sahel," EOS, Transactions, American Geophysical Union, 1993 Fall Meeting, Vol. 74(43):253.

Quarmby, N. A., J. R. G. Townshend, J. J. Settle, K. H. White, M. Milnes, T. L. Hindle and N. Silleos, 1992, "Linear mixture modelling applied to AVHRR data for crop area estimation," International Journal of Remote Sensing 13(3):415-425.

Raupach, M. R., 1992, "Drag and drag partition on rough surfaces," Boundary-Layer Meteorology 60:375-395.

Roberts, D. A. (1991), Separating spectral mixtures of vegetation and soils, Ph.D. dissertation, University of Washington, 180 pp.

Roberts, D. A., M. O. Smith, and J. B. Adams, 1993, "Green vegetation, nonphotosynthetic vegetation, and soils in AVIRIS data," Remote Sensing of Environment 44: 255-269.

Sabol, D. E., J. B. Adams, and M. O. Smith, 1992, "Quantitative sub-pixel spectral detection of targets in multispectral images," Journal of Geophysical Research 97:2659-2672.

Schlesinger, W. H., J. F. Reynolds, G. L. Cunningham, L. F. Huenneke, W. M. Jarrell, R. A. Virginia and W. G. Whitford, 1990, "Biological feedbacks in global desertification," Science, 247:1043-1048

Sellers, P. J., Y. C. Sud and A. Dalcher, 1986, "A simple biosphere model (SiB) for use within general circulation models," Journal of the Atmospheric Sciences 43(6): 505-531.

Sellers, P. J., S. I. Rasool and H.-J. Bolle, 1990, "A review of satellite data algorithms for studies of the land surface," Bulletin American Meteorological Society 71(10):1429-1447.

Sellers, P., F. G. Hall, G. Asrar, D. E. Strebel and R. E. Murphy, 1992, "An overview of the First International Satellite Land Surface Climatology Project (ISLSCP) Field Experiment (FIFE), Journal of Geophysical Research 97 (D17): 18345-18373.

Smith, M. O., S. L. Ustin, J. B. Adams and A. R. Gillespie, 1990, "Vegetation in deserts: I. A regional measure of abundance from multispectral images," Remote Sensing of Environment 31: 1-26.

Tucker, C. J., 1979, "Red and photographic infrared linear combinations for monitoring vegetation," Remote Sensing of Environment 8: 127-150.

Tuzet, A., J. F. Castell, A. Perrier and O. Zurfluh, 1993, "Transfer characteristics in sparse canopy cover," EOS, Transactions, American Geophysical Union, 1993 Fall Meeting, Vol. 74(43):232.

Van Leeuwen, S. J. D., A. R. Huete, J. Duncan and J. Franklin, 1994, "Radiative transfer in shrub savanna sites in Niger--First results of HAPEX-Sahel. 3. Optical dynamics and vegetation index sensitivity to biomass and plant cover," Agriculture and Forest Meteorology 69: 267-288.

Warren, P., and C. Dunford, 1986, "Sampling semiarid vegetation with large-scale aerial photography," ITC Journal, 4, 273-279.

Woodcock, C. E. and V. J. Harward, 1992, "Nested-hierarchical scene models and image segmentation," International Journal of Remote Sensing 13: 3167-3187.

Woodcock C. E., J. Collins, S. Gopal, V. Jakabhazy, X. Li et al., "Mapping forest vegetation using Landsat TM imagery and a canopy reflectance model," Remote Sensing of Environment, submitted.

X. Li and A. H. Strahler, 1986, "Geometric-optical bidirectional reflectance modeling of a conifer forest canopy," IEEE Transactions on Geoscience and Remote Sensing GE-24: 906-919.

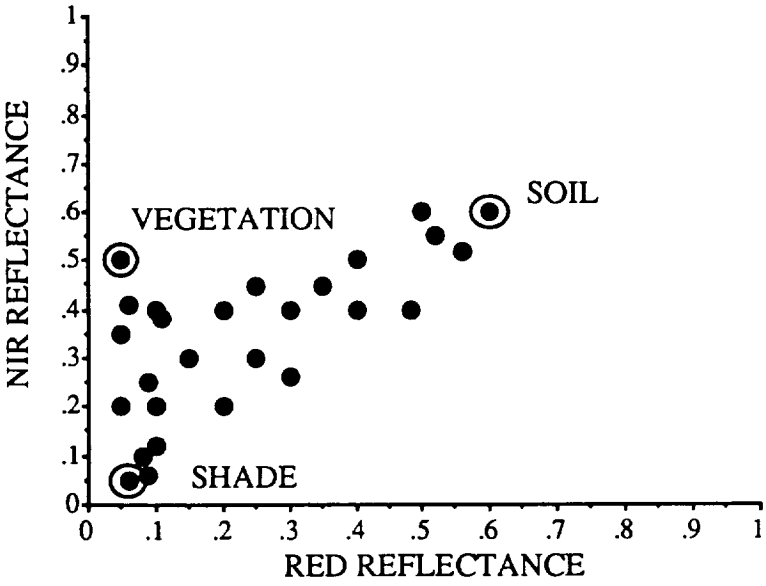

Figure 1.
Cartoon illustrating, in two dimensional spectral space, the theoretical positions of three endmembers: bright soil, green vegetation and shade.

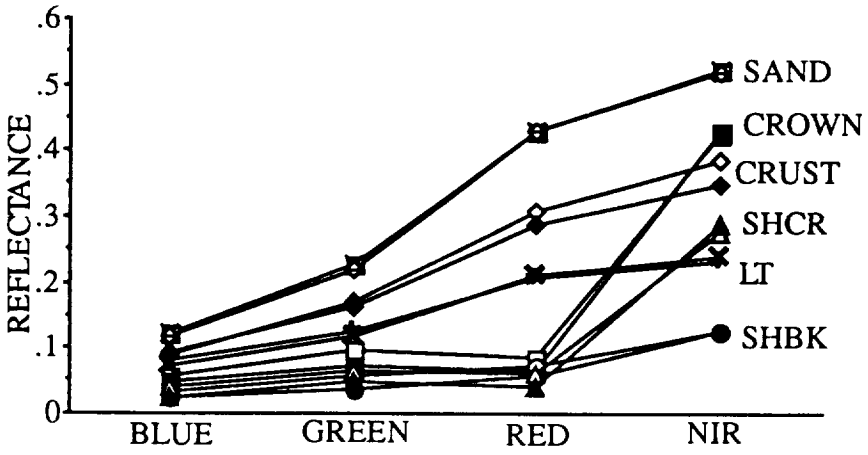

Figure 2.
Component spectra: SHCR=shadowed crown, LT=laterite, SHBK=shadowed background; 2 sample dates, DOY 212 (open symbols), DOY 280 (closed symbols).

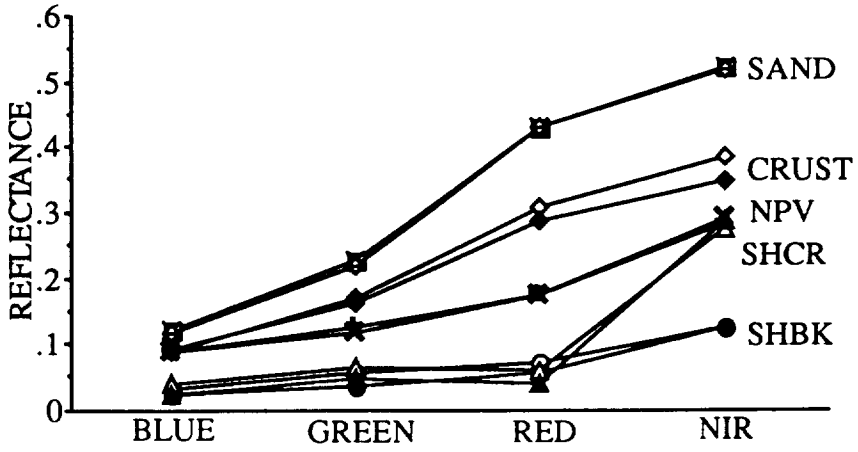

Figure 3.
Component spectra: Figure 2 is similar to Figure 1 with the addition of NPV=non-photosynthetically active vegetation and deletion of crown and LT (laterite).

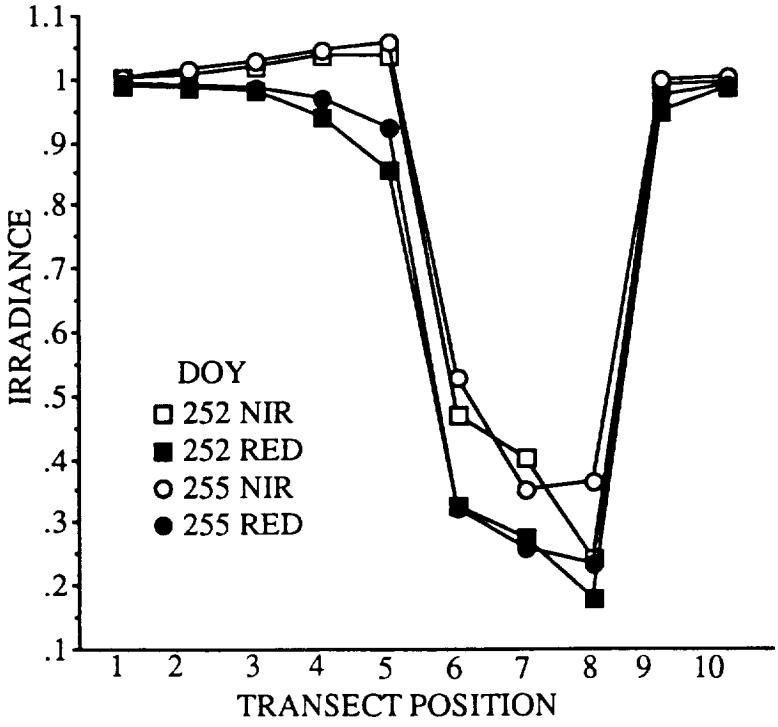

Figure 4.
Proportional spectral irradiance near and under Guiera shrubs: Transect positions (fully described in the text): positions 1-4 in the sun approaching the shrub, 5 is shrub edge, 6 and 7 are under shrub, 8 in shrub shadow, 9 and 10 in sun beyond shrub.

SPECTRAL MIXTURE/GEOMETRIC OPTICAL MODELING OF SURFACE COMPONENTS IN A SEMIARID REGION

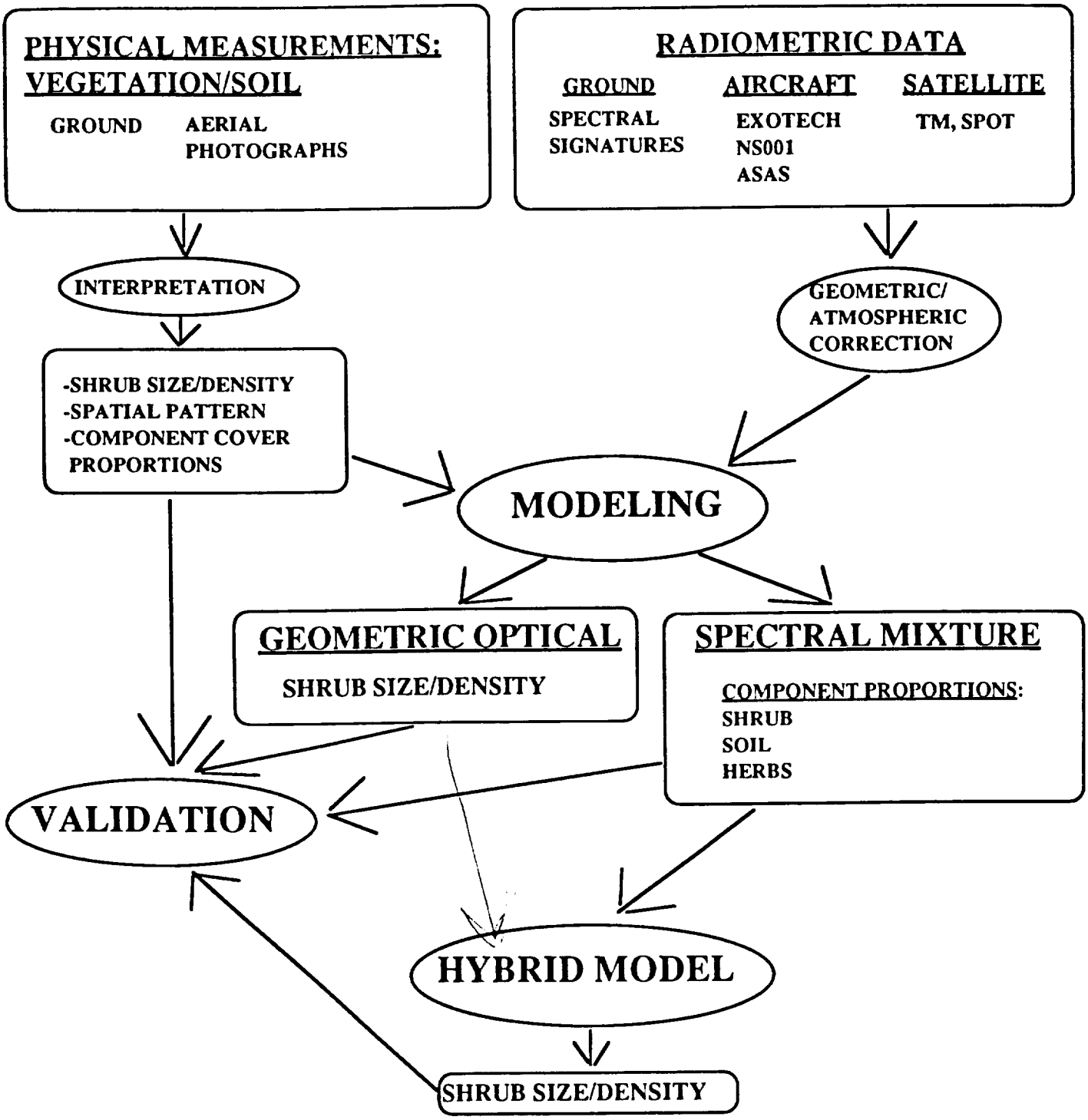

Figure 5